



Evaluation of long term Northern Hemisphere snow water equivalent products

Colleen Mortimer¹, Lawrence Mudryk¹, Chris Derksen¹, Kari Luojus², Ross Brown¹, Richard Kelly³, and Marco Tedesco⁴

5 ¹Climate Research Division, Environment and Climate Change Canada, Toronto, Canada

²Finnish Meteorological Institute, Helsinki, Finland

³Department of Geography and Environmental Management, University of Waterloo, Canada

⁴Lamont Doherty Earth Observatory, Columbia University, Palisades NY; NASA Goddard Institute for Space Studies, New York, USA

10 *Correspondence to:* Colleen Mortimer (colleen.mortimer@canada.ca)

Abstract. Seven gridded northern hemisphere snow water equivalent (SWE) products were evaluated as part of the European Space Agency (ESA) Satellite Snow Product Inter-comparison and Evaluation Exercise (SnowPEX). Three categories of datasets were assessed: (1) those utilizing some form of reanalysis (the NASA Global Land Data Assimilation System version 2 - GLDAS; the European Centre for Medium-Range Forecasts interim land surface reanalysis – ERA-land; the NASA
15 Modern-Era Retrospective Analysis for Research and Applications - MERRA; the Crocus snow model driven by ERA-Interim meteorology – Crocus); (2) passive microwave remote sensing combined with daily surface snow depth observations (ESA GlobSnow v2.0); and (3) standalone passive microwave retrievals (NASA AMSR-E historical and operational algorithms) which do not utilize surface snow observations. Evaluation included comparisons against independent surface observations from Russia, Finland, and Canada, and calculation of spatial and temporal correlations in SWE anomalies. The standalone
20 passive microwave SWE products (AMSR-E historical and operational SWE algorithms) exhibit low spatial and temporal correlations to other products, and RMSE nearly double the best performing product. Constraining passive microwave retrievals with surface observations (GlobSnow) provides comparable performance to the reanalysis-based products; RMSEs over Finland and Russia for all but the AMSR-E products is ~50 mm or less. Using a four-dataset ensemble that excluded the standalone passive microwave products reduced the RMSE by 10 mm (20%) and increased the correlation by 0.1; ensembles
25 that contain Crocus and/or MERRA perform better than those that do not. The observed RMSE of the best performing datasets is still at the margins of acceptable uncertainty for scientific and operational requirements; only through combined and integrated improvements in remote sensing, modeling, and observations will real progress in SWE product development be achieved.



30 1 Introduction

Temporally (~20–30 years) and spatially (~10–20 km) consistent estimates of daily SWE over seasonal snow covered land are required for many applications including climate model evaluation (Mudryk et al., 2018a), verification of seasonal forecasts (Sospedra-Alfonso et al., 2016), annual updates to climate assessments (e.g. Mudryk et al., 2018b; 2019), and determination of freshwater availability (Barnett et al. 2005; Clark et al. 2011). There are a growing number of gridded SWE datasets
35 available to the snow community, but these are typically affected by one or more critical shortcomings related to:

1. Challenges in using point measurements: Meaningful spatially continuous information can be derived from surface observations for regions and time periods with a sufficiently dense observing network (Dyer and Mote, 2006; Brown and Derksen, 2013); as an alternative to snow depth, surface snowfall measurements can also be integrated (Broxton et al., 2016). However, both snow depth and snowfall measurements from single point locations are intrinsically limited by a lack of
40 confidence in how they capture the landscape mean across coarse grid cells and surrounding areas that are not sampled, which is particularly problematic in areas of mixed forest vegetation, open areas prone to wind redistribution, and complex topography (most snow covered regions fall into at least one of these categories). Furthermore, there remain expansive alpine and northern regions with insufficient coverage by conventional observing networks (Brown et al., 2019).

2. Reliance on models driven by atmospheric reanalysis: Most modern reanalysis products include output of land surface variables such as SWE (Balsamo et al., 2015; Gelaro et al., 2017); alternatively the meteorology from these datasets can be
45 used to force snow models (Brown et al., 2003; Brun et al., 2013). While these snow schemes are of varying complexity, they typically do not account for important processes such as snow-vegetation interactions and redistribution by blowing snow. In addition, the spread in SWE estimates among differing reanalyses is large: not only do differences between snow models introduce uncertainties (Mudryk et al., 2015), but model-based approaches are also sensitive to the precipitation forcing, which
50 itself is challenging to validate in complex terrain and observation sparse regions (Lundquist et al., 2015; Henn et al., 2018). There may also be temporal inconsistencies in the forcing data related to changes in the observational streams assimilated in the reanalyses.

3. Coarse spatial resolution: Whether derived from passive microwave satellite measurements or some form of model reanalysis, the typical resolution of existing gridded SWE datasets is 25 to 100 km. While synoptic scale patterns can be
55 resolved at this resolution, spatial variability in SWE due to topographic and land cover heterogeneity is not adequately captured. Coarse resolution is a particularly critical limitation in alpine regions, which are masked out completely in some products (e.g. Takala et al., 2011). While this is a reasonable decision for coarse resolution products, it nevertheless is a source of frustration for users. Regional climate models can provide higher resolution SWE information, but the computational cost related to complex atmospheric physics schemes is, at least at present, a limiting factor in producing long time series (Wrzesien



60 et al., 2018). Coarse resolution also makes validation of SWE products challenging: the validation of large grid cells with single point measurements is conceptually unsatisfying and statistically non-robust.

4. Inability of remote sensing data to constrain uncertainty: The number of purely satellite derived SWE datasets is limited, and uncertainty in standalone passive microwave retrievals can be high (Kelly et al., 2003). The combination of passive microwave and surface snow depth measurements (within the GlobSnow product; Takala et al., 2011) was shown to yield
65 performance similar to snow models driven by atmospheric reanalysis (Mudryk et al., 2015), but it relies heavily on background fields and constraints generated from re-gridded surface snow depth observations (Pulliainen, 2006). The microwave remote sensing community has made great progress in understanding and quantifying error sources (snow microstructure, deep snow, wet snow, vegetation, lake ice), all of which are exacerbated by the coarse resolution of passive microwave measurements (Foster et al., 2005; Durand et al., 2011; Lemmetyinen et al., 2011; Durand and Liu, 2012).

70 Previous studies have demonstrated the potential for using multi-product SWE ensembles in order to improve estimates of observed snow-related quantities (e.g. SWE and snow cover fraction fields, integrated snow mass, snow cover extent and trends in these quantities) and to constrain uncertainty (Mudryk et al., 2015, 2017, 2018a; Krinner et al., 2018). The intent in such a strategy is that uncorrelated errors between products of the same type would average out, so the limitations and shortcomings of a given class of products would offset one another. Ideally such ensembles would draw from as many types
75 of products as possible and use multiple versions of each type of product. To date, these ensembles have relied heavily on models driven by atmospheric analysis and include only a single dataset (GlobSnow) which utilizes remote sensing. While SWE or snow depth products can be derived using InSAR techniques (Deeb et al., 2011) and airborne LiDAR data (Painter et al., 2016), such products are only available for regionally and temporal limited domains. Hence, the long time series of passive microwave measurements provide the most straightforward pathway to increase the use of satellite data within observational
80 SWE ensembles. Before existing passive microwave derived SWE products can be included, however, an assessment is needed because of markedly different climatological patterns (Fig. 1; discussed further in Sect. 3.1). The specific objectives of this study are to evaluation gridded Northern Hemisphere SWE products through (1) comparison with independent surface observations, and (2) calculation of the spatial and temporal correlations in SWE anomalies.



85

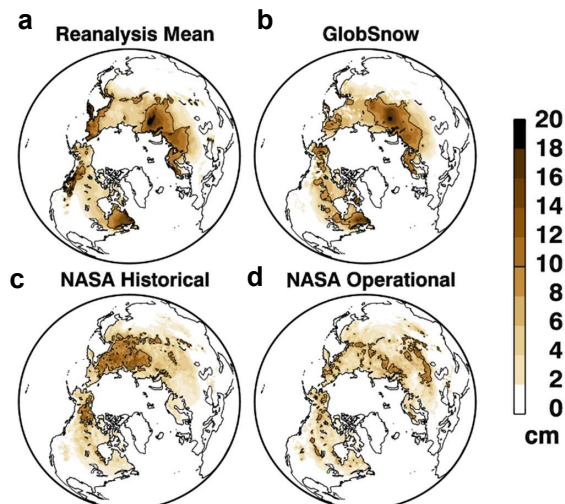


Figure 1. Mean January, February, and March (JFM) SWE over the 2003-2010 period for (a) four reanalysis driven products (GLDAS-2, ERA-interim-land, Crocus, and MERRA); (b) GlobSnow v2.0; (c) the historical NASA AMSR-E product; (d) the current operational NASA AMSRE-E algorithm.

90 2 Datasets

We evaluate three categories of northern hemisphere gridded SWE products: (1) standalone passive microwave retrievals (AMSR-E historical and operational algorithms); (2) passive microwave estimates combined with surface snow depth observations (GlobSnow), and (3); products which utilize some form of reanalysis (Crocus, ERA-land, GLDAS-2, MERRA).

1. *Standalone passive microwave:* The NASA historical AMSR-E product
95 (https://nsidc.org/data/AE_DySno/versions/2, Tedesco et al. 2004) is described in Kelly (2009) and evaluated in Tedesco and Narvekar (2010). Brightness temperature thresholds are utilized to identify shallow and non-shallow dry snow areas, with the depth of shallow snow set to 5 cm (Kelly et al., 2003). SWE is retrieved based on a brightness temperature difference approach (37-19 GHz; based on the original formulation of Chang et al. (1990)) with enhancements to account for the influence of vegetation, address deeper snowpacks (through the use of 10 GHz measurements), and consider the dynamic influence of snow grain size (based on the assumption that as snow depth increases, the depth average grain size increases). Snow depth is converted to SWE using the snow climate classification of Sturm et al. (1995) and snow density climatologies from Brown and Braaten (1998) and Krenke (2004). Building on the historical AMSR-E SWE product, NASA's current 'operational' AMSR-E SWE algorithm utilizes an artificial neural network (ANN), snow emission modelling, and climatological snow depth data for the
100



- 105 estimation of snow depth, and the detection of dry versus wet snow conditions (Tedesco and Jeyaratnam 2016). Snow
density maps based on Sturm et al. (2010) are employed for conversion of retrieved snow depth to SWE. Unlike the
GlobSnow approach described next, both the operational and historical AMSR-E algorithms are self-contained and
do not rely on any external temporally variable snow measurements.
- 110 2. *Synergistic passive microwave + in situ*: The European Space Agency GlobSnow v2.0 SWE product (data available
at www.globsnow.info) is based on a retrieval method first described in Pulliainen (2006). The approach evolved
from standalone passive microwave algorithms in that it also relies on the channel difference between 19 and 37 GHz
measurements, but the retrieval also integrates daily surface snow depth measurements. First, daily climate station
snow depth observations are kriged to form a continuous background field independent of passive microwave
retrievals. This first guess snow depth field is used as input to two iterations of forward microwave emission model
115 simulations, one to estimate grain size, the second to estimate snow depth (Takala et al., 2011). A temporally and
spatially fixed snow density value of 0.24 g cm^{-3} is applied to convert snow depth to SWE. Alpine areas are excluded
due to known limitation of this technique in regions with complex sub-grid topographical heterogeneity (Takala et
al., 2011).
- 120 3. *Land surface models and reanalysis*: Four SWE datasets derived from combinations of land surface models driven
by reanalysis meteorology were used for comparison with the passive microwave products: the NASA Global Land
Data Assimilation System version 2 - GLDAS; the European Centre for Medium-Range Forecasts interim land
surface reanalysis – ERA-land; the NASA Modern-Era Retrospective Analysis for Research and Applications -
MERRA; the Crocus snow model driven by ERA-interim meteorology – Crocus. A full description of the derivation
of SWE from these products is provided in Mudryk et al. (2015). Differences in both the forcing data and the snow
125 schemes (which are of varying complexity) within the land surface models account for spread between these products
(see Mudryk et al., 2015). For example, both Crocus and ERA-land use the same forcing data but employ different
land models with different snow schemes. Henceforth, we refer to these datasets as *snow analyses*.

A summary of the seven SWE datasets used in this study is provided in Table 1. All datasets were interpolated to a regular 1°
 $\times 1^\circ$ longitude–latitude grid. Before interpolation, snow over glaciers and large lakes was excluded based on the MERRA land
130 fraction mask (consistent with Mudryk et al., 2015).



135 **Table 1.** Summary of SWE products evaluated in this study.

Dataset	Method	Ancillary/ Forcing Data	Resolution	Time Series	Reference
GlobSnow v2.0	Passive microwave + in situ	Weather station snow depth measurements	25 km	1979-2015	Takala et al (2011)
NASA AMSR-E historical	Standalone passive microwave		25 km	2002-2011	Kelly (2009)
NASA AMSR-E operational	Microwave + ground station climatology	Weather station snow depth climatology	25 km	2002-2011	Tedesco and Jeyaratnam (2016)
ERA-land	HTESSEL land surface model	ERA-interim	0.75° x 0.75°	1981-2010	Balsamo et al (2013)
MERRA	Catchment land surface model	MERRA	0.5° x 0.67°	1981-2010	Rienecker et al (2011)
Crocus	ISBA land surface + Crocus snow model	ERA-interim	1° x 1°	1981-2010	Brun et al (2013)
GLDAS-2	Noah 3.3 land surface model	Princeton Met.	1° x 1°	1981-2010	Rodell et al (2004)

2.1 Snow course data

140 Snow course data (which are fully independent of the point snow depth measurements assimilated into GlobSnow) were acquired for evaluation of the gridded SWE products. While more limited in number than snow depth observations, these transect measurements provide better consideration of sub-grid scale variability not available from operational snow depth networks which provide only single point measurements of snow depth.

145 Russia has a long-term snow course network located near 517 meteorological stations (Bulygina et al., 2011). The snow survey transects extend for 1 to 2 km in open areas, and 500 m at forested sites. Measurements are made every ten days when at least half of the visible area around a station is snow-covered, except at forested sites where measurements are made once per month prior to 20 January. Sampling frequency is increased to five days during the spring snow melt season. The Finnish snow course network, maintained by the Finnish Environment Institute (SYKE), consists of approximately 200 transects distributed across



the country. Measurements are conducted monthly around the 15th of each month, with a subset of snow courses also measured at the end of each month. Each snow course is 2 to 4 km long, and extends through variable land cover consistent with the surrounding landscape.

150 Canadian snow course data were acquired from a recently updated collection of national and regional networks described in Brown et al. (2019). There is no comprehensive national strategy in Canada to obtain a spatially representative collection of snow course measurements. Snow courses are maintained by various jurisdictions resulting in a spatially heterogeneous sample distribution heavily biased towards population centres. For 2002 through 2010, there were >1000 different snow course locations with varying sampling frequency. Measurements are typically made around the 1st and 15th of each month during the
155 snow season (November to April). Snow courses are roughly 150 to 300 m long consisting of five to ten sampling locations (Brown et al., 2019). While the network density is very sparse across Canada, and the transects are much shorter in length than the Russian and Finnish data, the measurements still capture reasonable landscape mean values (Neumann et al., 2006).

The snow course observations were converted into bi-weekly gridded datasets. Observations were grouped into bi-weekly periods using a 16 day window centred on the 1st or 15th of each month. Over Russia, observations were grouped into ten day
160 periods corresponding to the typical measurement dates (10th, 20th, 30th of each month). For each time step, the average of all snow course measurements within a 25 x 25 km EASE2 grid cell was obtained. Validation statistics in Sect. 3.2 are reported for this gridded dataset.

3 Results

3.1 Climatology

165 There is notable disagreement in the climatological SWE distribution over the northern hemisphere land area between standalone passive microwave products and the other data sources (Fig. 1). The pattern of high and low SWE between western and eastern Siberia is reversed for the four snow analyses and GlobSnow versus the two AMSR-E algorithms. This inconsistency across Eurasia was also evident in analysis of older versions of passive microwave derived SWE data (e.g. Rawlins et al., 2007), reanalysis, and climate model simulations (see Fig. 2 in Clifford et al., 2010). The AMSR-E products
170 also fail to capture a pronounced region of high SWE in eastern Canada present in the other datasets. The GlobSnow climatology is in close agreement with the snow analyses, particularly over Eurasia. The four snow analyses and GlobSnow also agree with other SWE climatologies derived from other sources covering different time periods and thus not included in this study (see Brown and Mote, 2009; Liston and Hiemstra, 2011).

The difference in climatological SWE patterns is not solely due to the well-documented systematic underestimation in passive
175 microwave retrievals when SWE exceeds 150 mm (Markus et al., 2006). Eastern Siberia is a low winter-season precipitation environment with very cold surface temperatures. These are ideal conditions for a thin, low density snowpack (see Liston and



Hiemstra, 2011), likely composed primarily of faceted snow grains due to kinetic metamorphism, as seen in the Canadian Arctic (Derksen et al., 2014) and Alaskan North Slope (Hall, 1987). Thin snow composed of large faceted grains results in exaggerated scattering relative to the amount of SWE (Hall et al., 1991), hence the comparatively large SWE estimates for the standalone passive microwave products.

The source of inability of the standalone passive microwave products to capture higher SWE in western Siberia, Russia, northern Europe, and eastern Canada is less clear, but may be related to weaker scattering signatures from smaller grained and deeper snow, which is further masked by microwave emission from forest cover. The ability of GlobSnow to retain sensitivity to deeper snow than the AMSR-E products is due to the assimilation of daily surface snow depth observations which work to ‘nudge’ the retrievals to higher values (Pulliainen, 2006). In observation sparse regions such as northern Quebec, the GlobSnow retrieval must rely more on the passive microwave retrievals, which increases uncertainty in these areas (Larue et al., 2017; Brown et al., 2018) compared to forested, deep snow regions with a dense observation network such as Finland (Takala et al., 2011).

3.2 Comparison with Surface Measurements

The seven SWE datasets were compared to Canadian, Finnish, and Russian snow course measurements for all snow seasons (November–April) over the November 2002 to April 2010 period. The results are summarized by each national snow course dataset in order to separate any sensitivity to differences in snow course measurement protocol and sample distribution. Statistics were computed for SWE product grid cells matched up in space and time with the gridded snow course measurements (Sect. 2.1). To permit comparison between products, only grid cells with coincident values from all seven SWE products were retained. Mountain areas were excluded from the analysis because they are masked in GlobSnow. A summary of the validation results is provided in Fig. 2.

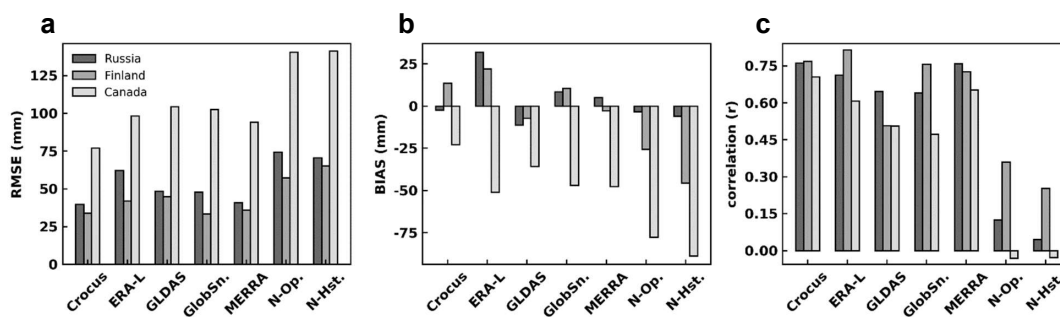


Figure 2. Validation statistics (a: RMSE; b: Bias; c: correlation) for the seven SWE products for November through April, 2002–2010. N-Op. and N-Hst. refer to the AMSR-E operational and historical products, respectively.



All products exhibit weaker skill over Canada, where the RMSE for all products is roughly twice that of Finland and Russia. Larger absolute bias and RMSE over Canada may be attributed, in part, to a higher average SWE (mean of all snow course observations > 140 mm compared to < 100 mm for both Finland and Russia). Performance of the standalone passive microwave products (AMSR-E) is noticeably weaker for all regions and validation statistics with the exception of bias over Russia. Crocus had the smallest RMSE and bias and strongest correlation over both Canada and Russia. Over Finland and Russia, all except the AMSR-E products have RMSE values of approximately 50 mm or less, with the exception of ERA-land over Russia. RMSE for the standalone passive microwave products is nearly double that of the best performing product for both Finland and Canada, with slightly better results over Russia. For Finland and Russia, bias ranged between ± 15 mm for all datasets except ERA-land and the standalone passive microwave products. Over Canada, bias ranged from -23 to -51 mm for all but the AMSR-E products (-78 to -89 mm). Correlation coefficients for all but the standalone passive microwave products was ~ 0.5 and greater. The AMSR-E products exhibited lower or even negative correlations with snow course measurements for all three reference datasets.

We find that among GlobSnow, Crocus, ERA-land, GLDAS, and MERRA no individual product performs *best* with respect to the RMSE, bias, and correlation statistics across all regions. This is an important finding, as it shows no clear advantage to using a single type of snow analysis, whether it is remote sensing combined with surface observations, an external snow model driven by reanalysis meteorology, or the land surface schemes within reanalyses. With higher RMSEs, greater bias, and weaker correlations relative to the other five datasets, this assessment raises concerns about the ability of current standalone passive microwave algorithms to perform in a comparable fashion to the other products. It is important to note that the RMSE of the best performing products is at the margins of acceptable uncertainty for operational and scientific requirements (Rott et al., 2010; Larue et al. 2017; Derksen and Nagler, 2019).

To determine the influence of SWE magnitude on product performance, all three reference snow course datasets were binned into 10 mm increments for comparison with the gridded SWE estimates (Fig. 3). Crocus and MERRA perform in a similar fashion, with reasonable agreement up to about 150 mm of SWE and a tendency to under (over) estimate SWE for deeper (shallow) snow. The performance of GLDAS and GlobSnow is similar to Crocus and MERRA, except that GLDAS underestimates SWE across a larger range of reference values (above ~ 100 mm), consistent with the negative bias in Fig. 2b, while GlobSnow overestimates SWE up to ~ 100 mm. ERA-land overestimates SWE up to ~ 180 mm, consistent with the positive bias over Russia and Finland (Fig. 2b). The historical AMSR-E product exhibits low sensitivity to SWE, especially for values > 60 mm and overestimates low SWE values. Better results were found for the newer AMSR-E operational algorithm, although the retrievals plateau at about 100 mm, and show no sensitivity to further SWE increases.

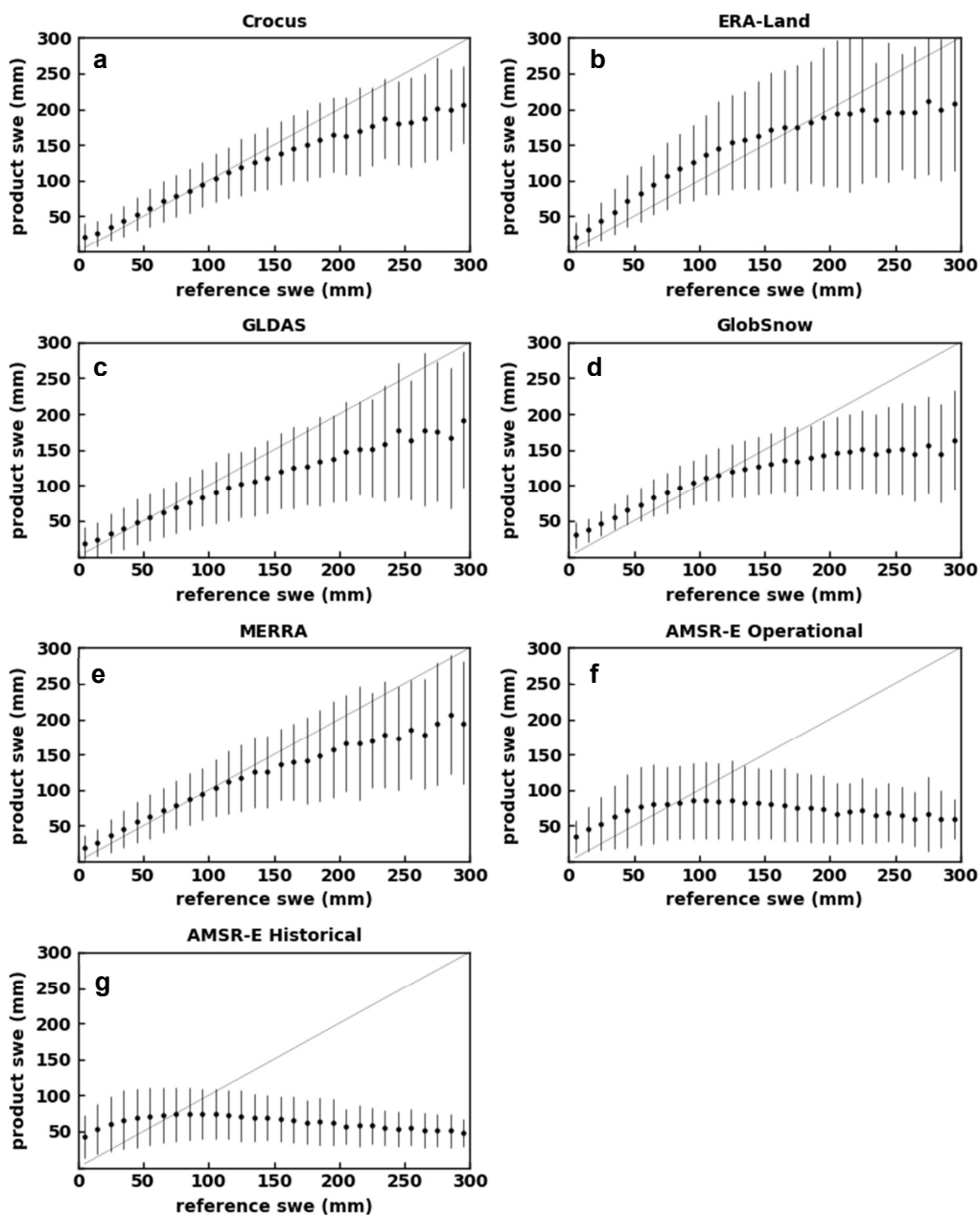


Figure 3. Retrieval performance versus reference SWE \pm 1 standard deviation for (a) GlobSnow; (b) Crocus; (c) GLDAS; (d) MERRA; (e) ERA-Land; (f) AMSR-E historical; (g) AMSR-E operational. SWE values above 300 mm are not shown.



235 To quantify the influence of seasonality on product performance, validation statistics (RMSE, bias, correlation) were computed
at a bi-weekly time step for 2002 through 2010. Figure 4 shows the monthly evolution from November through April over
Russia and provides insight into both the seasonal evolution of product-specific uncertainty, and the spread in uncertainty
between products. In general, RMSE and bias both increase over the course of the snow season. Early in the snow season, the
RMSE and bias are low because snow is shallow, although even small errors can produce high relative RMSE. As SWE
240 increases through the snow accumulation season, the RMSE magnitude and the spread in RMSE between products increases.
Bias becomes increasingly negative over the course of the snow season with the notable exception of ERA-land (over Russia)
which trends towards larger positive values. This is consistent with anomalously high SWE in ERA-land over Eurasia reported
elsewhere (Mudryk et al., 2015). Toward the end of the snow season, inter-product spread in the error statistics are at a
maximum. Peak uncertainty late in the season is driven by cumulative errors over the entire season, differences in the timing
245 of snow onset, and different melt rates. Whereas the RMSE and bias evolve over the course of the snow season, the magnitude
of correlation for all but the AMSR-E products is stable. This is an encouraging result as it indicates that SWE anomalies
should be reasonably realistic throughout the season, even if climatological amounts of SWE differ strongly between analyses.
A similar seasonal evolution of product specific uncertainties is observed for both Finland and Canada (not shown).

As with the bulk comparison to the snow course measurements summarized in Fig. 2, and the summaries of product
250 performance versus SWE magnitude in Fig. 3, Crocus and MERRA appear to perform slightly better than the other reanalysis-
based products and GlobSnow, while the two AMSR-E products exhibit a greater degree of uncertainty. Crocus tends to have
biases near zero and a low RMSEs for most regions and time steps as does MERRA, except late in the snow season.



255

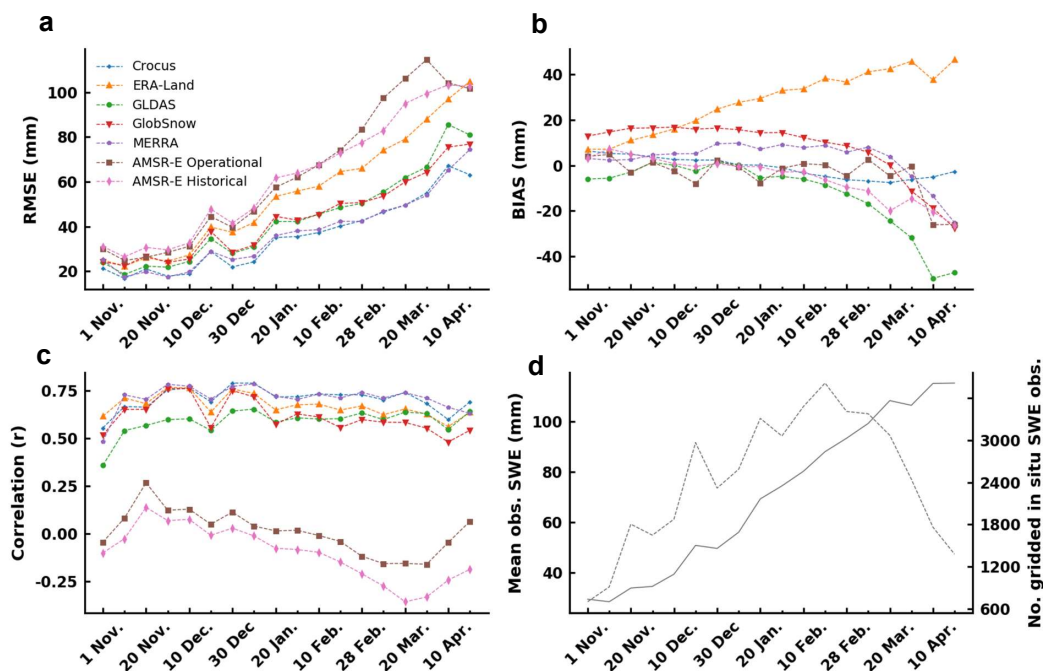


Figure 4. (a) RMSE, (b) bias and (c) correlation coefficient relative to the Russia snow course dataset (Sect. 2.1) for each ten-day time step over the 2002-2010 period. (d) Solid line: mean SWE value over all Russian snow course measurements for each time step; dashed line: number of Russian gridded snow course observations.

Given that no one product is always the best performer with respect to error statistics and regions analysed, we investigated the effect of using multi-product SWE ensembles to minimize uncertainty (e.g. Mudryk et al., 2015, 2017, 2018a; Krinner et al., 2018). The two AMSR-E products were excluded from this comparison because of the low correlation with snow course measurements as illustrated in Figs. 2c, 3f, 3g, and 4c. As the number of products included in a given inter-product ensemble increases, the correlation improves and the RMSE decreases (Fig. 5b). The level of improvement, however, saturates when four products are included in the ensemble. In addition, ensembles that contain contain Crocus and/or MERRA perform better than those that do not (Fig. 5a). This suggests that although there is no single best product, there are some products (Crocus and MERRA) that should be included in any multi-product mean. Importantly, four- and five- product ensembles that include Crocus and MERRA have higher (lower) correlation (RMSE) with snow course measurements compared to that of any individual product.

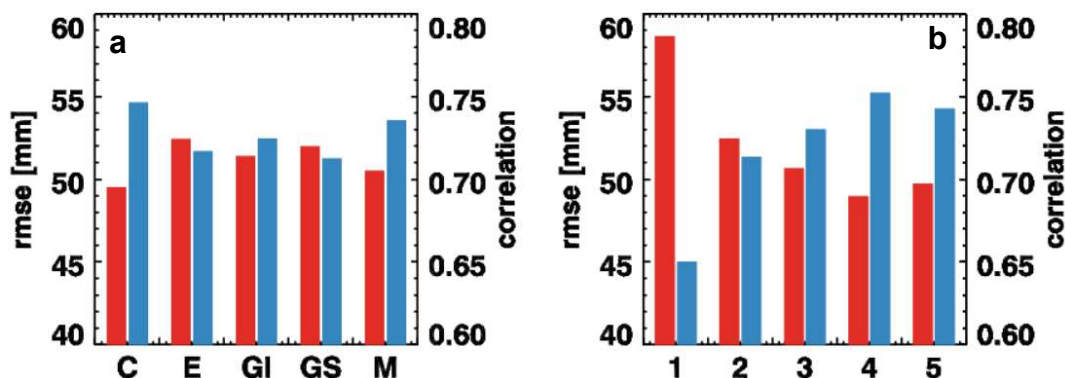


Figure 5. RMSE (red) and correlation (blue) of snow course measurements with various combinations of SWE products. (a) Average of all combinations that contain the specified individual product [C = Crocus, E = ERA-Land, GI = GLDAS, GS = GlobSnow, M = MERRA] and (b) average of all combinations of N products as specified on x-axis.

275 3.3 Correlation Analysis

To determine the strength of agreement among datasets, two types of pairwise correlations were calculated. Temporal correlations were calculated for time series of daily northern hemisphere snow mass (SWE integrated over the land area). A value was determined for each pair of datasets by correlating the two snow mass anomaly time series for all winter days (November–April (NDJFMA)) over the 2003–2010 period. Spatial correlations were calculated for a given dataset pair by averaging the sequence of pattern correlations of anomalous daily SWE calculated for all winter days (NDJFMA) over 2003–2010. Both anomalous SWE fields and anomalous snow mass were calculated for each dataset using its respective 2003–2010 climatology. Calculated as such, these correlations reflect both intra-seasonal and inter-annual covariance.

In all cases, the mean pattern correlation is lower than the corresponding temporal correlation of total snow mass (Fig. 6). This result may be due to the presence of opposite-signed spatial biases that cancel when spatially aggregated into a snow mass time series. The four datasets which rely on reanalysis in some way (Crocus, GLDAS, MERRA, ERA-land) exhibit a moderately strong spatial and temporal correlation with each other. These correlations range between 0.5 and 0.7 (illustrated in the R4 symbols in Fig. 6), and represent the average of the six pairwise combinations of these four products. The agreement among these four datasets is expected since ERA-land and Crocus both use the same forcing meteorology (Table 1), and the ERA meteorology is itself well correlated with that of MERRA and GLDAS. GlobSnow, which is completely independent from the products using reanalysis, is reasonably well correlated (especially the temporal correlations) with the R4 products (illustrated in the GS symbols in Fig. 6). There is a lack of temporal and spatial correlation between the AMSR-E products and the R4 datasets. Spatially, this is an expected result given the differences in climatological SWE patterns shown in Fig. 1. The



weak temporal correlation means the SWE anomalies do not evolve in-phase with the other products as the snow season evolves.

295

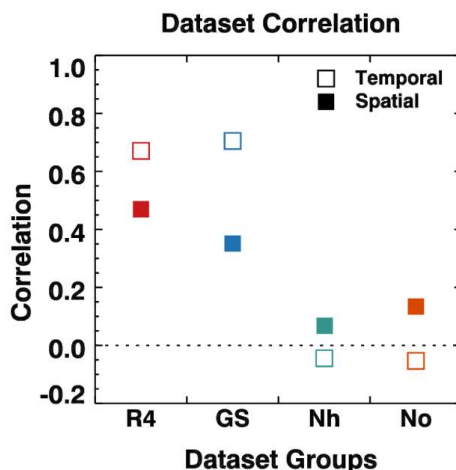


Figure 6. Representative values for temporal and spatial correlations among groups of products over the 2003–2010 time period. (Temporal correlations assess the extent to which total northern hemispheric snow mass jointly evolves between pairs of datasets; spatial correlations assess the pattern correlation of SWE fields for pairs of datasets.) See text for details. R4 = the average of 6 pairwise correlations between Crocus, GLDAS, ERA-land, and MERRA. GS = the average of 4 pairwise correlations between GlobSnow and each R4 product. Nh = the average of 4 pairwise correlations between AMSR-E historical and each R4 product. No = the average of 4 pairwise correlations between AMSR-E operational and each R4 product.

Further insight is gained through the calculation of correlation maps among groups of datasets (Fig. 7), where temporal correlations of daily SWE are calculated as above but for each grid cell. As expected, the modern era reanalysis datasets are strongly correlated to each other (R4-R4 in Fig. 7). Correlations between GlobSnow and the R4 products are strong across most snow covered regions of the northern hemisphere (GS-R4), with the exception of parts of Arctic Canada and the ephemeral snow zones of both North America and Eurasia (note that alpine areas are masked in the GlobSnow product). As noted earlier, the performance of GlobSnow is closely tied to the density of snow depth data used as inputs to the retrievals (Larue et al., 2017; Brown et al., 2018) which likely contributes to the low correlations in parts of Arctic Canada where there are relatively few snow depth observations. The NASA AMSR-E historical dataset exhibits very weak anomaly correlations with the R4 datasets (Nh-R4), and even negative correlations over the boreal forest of North America and parts of central and eastern Siberia. The AMSR-E operational algorithm shows improved anomaly correlations over eastern Siberia (No-R4; likely by better accounting for the combination of shallow snow and large snow grains found in this region (Tedesco and Jeyaratnam, 2016)) and the boreal forest of North America, although correlations remain weak over the remainder of the snow-covered northern hemisphere.



320

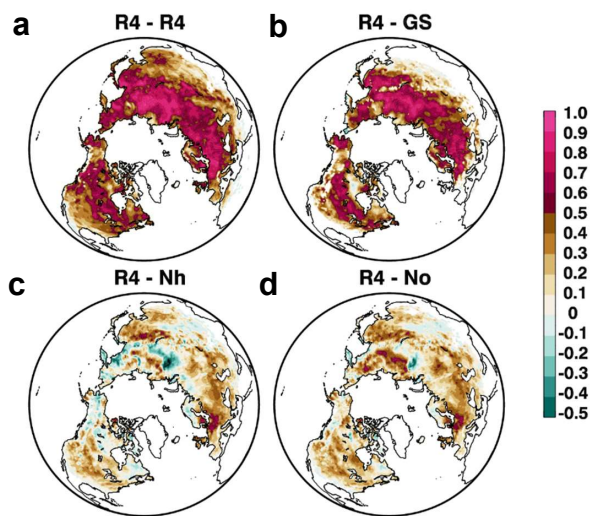


Figure 7. Correlation maps for four reanalysis driven products (Crocus, GLDAS-2, ERA-land, and MERRA) relative to: (a) each other (mean correlation between the four reanalysis driven products); (b) GlobSnow v2.0; (c) the NASA AMSR-E historical product; (d) the operational AMSR-E algorithm.

325 4. Conclusions and Discussion

In this study, we compared three types of northern hemisphere gridded SWE products: (1) those utilizing some form of reanalysis (Crocus, ERA-land, GLDAS, MERRA); (2) passive microwave remote sensing combined with surface observations (GlobSnow); and (3) standalone passive microwave retrievals (AMSR-E historical product and operational algorithm). There is past evidence of acceptable algorithm performance for standalone passive microwave products, particularly in open environments with relatively shallow snow (Derksen et al., 2004; Vuyovich et al., 2014), or when SWE retrievals are converted to snow cover extent (Brown et al., 2010). At the continental scale however, the standalone AMSR-E SWE products have stark differences in climatological SWE patterns compared to other available products (see Fig. 1).

Evaluation against snow course measurements from Russia, Finland, and Canada, show higher RMSE and bias, and lower correlation for standalone passive microwave products compared to the five other datasets (Fig. 2). While uncertainty for all products tends to increase with deeper snow, this is a critical issue for the AMSR-E products because of pronounced negative

335



bias even at relatively low SWE values (<100 mm; Fig. 3 and 4). Although there is no single best product with respect to bias, RMSE and correlation, there are some products, namely Crocus and MERRA, that should be included in any multi-product mean (Fig. 5). Correlation analysis performed with respect to both space and time shows consistent behaviour with strong statistical agreement among the four reanalysis-based products and GlobSnow (consistent with Mudryk et al., 2015), which
340 clearly benefits from the ingestion of daily surface snow depth data into the retrievals. The AMSR-E products exhibit weak spatial agreement and negative temporal anomaly correlations with the other datasets (Fig. 6 and 7).

The retrieval of SWE solely from passive microwave measurements is a difficult challenge, and despite the best efforts of many research groups over many decades, passive microwave - based standalone algorithms do not perform as well as other methods that make use of ancillary snow measurements. Although there are many attractive attributes (wide swath, all-weather
345 imaging, long legacy time series, and theoretical sensitivity to SWE under simplified assumptions) passive microwave data has always been a measurement of opportunity for snow applications, not an idealized measurement system. This introduces intrinsic biases and errors into the standalone retrieval scheme because of the non “optimal” nature of these measurements for snow applications.

Despite these challenges, there are opportunities to utilize satellite passive microwave measurement as a component of SWE
350 product development moving forward. Machine learning operators show great potential for the radiance-based assimilation of brightness temperatures (e.g. Forman and Reichle 2014) analogous to how L-band brightness temperatures are assimilated for improved soil moisture analyses. Assimilation approaches also show potential for addressing challenges posed by stratigraphy (Durand et al., 2011; Andreadis and Lettenmaier, 2012) and deep snow (Li et al., 2012). While coarse resolution is an inherent challenge with satellite passive microwave measurements, enhanced resolution products spanning multiple decades are now
355 available (Takala et al., 2017; Long and Brodzik, 2016).

The combination of brightness temperature measurements, surface snow depth observations, and forward radiometric modeling are able to produce skillful SWE products. This approach was already used successfully within the ESA GlobSnow project and it will be further enhanced within the ESA Climate Change Initiative (CCI) snow project. It is important to note that the brightness temperature component of the GlobSnow/Snow CCI retrieval has direct heritage to standalone passive
360 microwave retrieval approaches which date back to the first generation of passive microwave imagers launched in the 1970s. This also suggests that research focusing on passive microwave interactions with snow parameters should not be neglected as, ultimately, understanding the physics is a necessary step for algorithm improvement.

While the continued development of a remote sensing capability for SWE represents an important observational capability, it is necessary to also appreciate the quality of the large scale model derived SWE products. The combination of reanalysis
365 meteorology and snow models yields very useful snow information, which can be refined as forcing data (particularly



precipitation) and snow models continue to improve. Only through combined and integrated improvements in remote sensing, modeling, and observations will real progress in SWE product development be achieved.

Data availability. Eric Brun provided data from the Crocus snowpack model; the NASA AMSR-E operational dataset and is
370 available from the paper's authors upon request as is the NASA AMSR-E operational dataset. The remaining datasets are
available for download via the links and references provided in Sect. 2.

Competing interests. The authors declare that they have no conflicts of interest.

Acknowledgements. This work was conducted as a part of the European Space Agency funded Satellite Snow Product Inter-
comparison Exercise (SnowPEX). We appreciate the contributions from data providers: Météo-France (Crocus), NASA
375 Goddard Earth Sciences Data and Information Services Center (MERRA, GLDAS), European Centre for Mid-range Weather
Forecasts (ERA-Interim/Land), and the Finnish Meteorological Institute (GlobSnow). Snow course data were made available
by RusHydroMet, the Finnish Environment Institute (SYKE), and the Meteorological Service of Canada. Mike Brady (ECCC)
provided technical support and assistance. Thanks to the late Dr. Andrew Slater for inspiration.

References

380 Andreadis, K., and Lettenmaier, D.: Implications of representing snowpack stratigraphy for the assimilation of passive
microwave satellite observations, *J. Hydrometeorol.*, 13, 1493–1506, <https://doi.org/10.1175/JHM-D-11-056.1>, 2012.

Balsamo, G., Albergel, C., Beljaars, A. , Boussetta, S. , Brun, E. , Cloke, H. , Dee, D. , Dutra, E., Muñoz-Sabater, J.,
Pappenberger, F. , de Rosnay, P., Stockdale, T., and Vitart, F. : ERA-Interim/Land: a global land surface reanalysis data set,
385 *Hydrology and Earth System Science*, 19, 389–407, <https://www.hydrol-earth-syst-sci.net/19/389/2015>, 2015.

Barnett, T. P., Adam, J.C., and D.P. Lettenmaier, D. P.: Potential impacts of a warming climate on water availability in snow-
dominated regions, *Nature*, 438, 303–309. <https://doi.org/10.1038/nature04141>, 2005.

390 Baseman, J. and D. Fernandez-Prieto (eds.). ESA-CliC Earth Observation and Arctic Science Priorities. Tromso, Norway, 20
Jan 2015. <http://www.climate-cryosphere.org/media-gallery/1533-esa-clic-arctic-2015>, 2015.

Brown, R., and Braaten, R.: Spatial and temporal variability of Canadian monthly snow depths, 1946-1995, *Atmos.-Ocean*,
36, 37–54. <https://doi.org/10.1080/07055900.1998.9649605>, 1998.

395



- Brown, R., Brasnett, B., and Robinson, D.: Gridded North American monthly snow depth and snow water equivalent for GCM evaluation. *Atmos.-Ocean*, 41, 1–14. <https://doi.org/10.3137/ao.410101>, 2003.
- Brown, R., and Mote, P.: The response of Northern Hemisphere snow cover to a changing climate. *J. Climate*, 22, 2124–2145, 400 <https://doi.org/10.1175/2008JCLI2665.1>, 2009.
- Brown, R., Derksen, C., and Wang, L.: A multi-dataset analysis of variability and change in Arctic spring snow cover extent, 1967–2008. *J. Geophys. Res.*, 115, D16111, <https://doi.org/10.1029/2010JD013975>, 2010.
- 405 Brown, R., and Derksen, C.: Is Eurasian October snow cover extent increasing?, *Env. Res. Lett.*, 8, 024006, <https://doi.org/10.1088/1748-9326/8/2/024006>, 2013.
- Brown, R., Tapsoba, D. and Derksen, C.: Evaluation of snow water equivalent datasets over the Saint-Maurice river basin region of southern Québec. *Hydrol. Process.*, 32, 2748–2764, <https://doi.org/10.1002/hyp.13221>, 2018.
- 410 Brown, R. D., Fang, B. and Mudryk, L. Update of Canadian historical snow survey data and analysis of snow water equivalent trends, 1967-2016. *Atmos.-Ocean*, 57, 1–8, <https://doi.org/10.1080/07055900.2019.1598843>, 2019.
- Broxton, P. D., Dawson, N., and Zeng, X.: Linking snowfall and snow accumulation to generate spatial maps of SWE and 415 snow depth, *Earth and Space Science*, 3, 246–256, <https://doi.org/10.1002/2016EA000174>, 2016.
- Brun, E., Vionnet, V., Boone, A., Decharme, B., Peings, Y. , Vallette, R. , Karbou, F., and Morin, S.: Simulation of northern Eurasian local snow depth, mass, and density using a detailed snowpack model and meteorological reanalyses, *J. Hydrometeorol.*, 14, 203–219, <https://doi.org/10.1175/JHM-D-12-012.1>, 2013.
- 420 Bulygina, O., Groisman, P Ya, Razuvaev, V., and Korshunova, N.: Changes in snow cover characteristics over Northern Eurasia since 1966, *Env. Res. Lett.*, 6, 045204, <https://doi.org/10.1088/1748-9326/6/4/045204>, 2011.
- Chang, A., Foster, J., and Hall, D.: Satellite sensor estimates of northern hemisphere snow volume. *Int. J. Remote Sens.*, 11, 425 167–171. <https://doi.org/10.1080/01431169008955009>, 1990.
- Clark, M. P., Hendrix, J. , Slater, A. G. , Kavetski, D. , Anderson, B. , Cullen, N. J. , Kerr, T., Hreinsson, E. O., and Woods, R. A.: Representing spatial variability of snow water equivalent in hydrologic and land-surface models: a review, *Water Resour. Res.*, 47, W07539, <https://doi.org/10.1029/2011WR010745>, 2011.



430

Clifford, D.: Global estimates of snow water equivalent from passive microwave instruments: history, challenges and future developments. *Int. J. Remote Sens.*, 31, 3707–3726, <https://doi.org/10.1080/01431161.2010.483482>, 2010.

435 Deeb, E., Forster, R., and Kane, D.: Monitoring snowpack evolution using interferometric synthetic aperture radar on the North Slope of Alaska, USA, *Int. J. Remote Sens.*, 32, 3985–4003, <https://doi.org/10.1080/01431161003801351>, 2011.

Derksen, C., Brown, R., and Walker, A.: Merging conventional (1915–92) and passive microwave (1978–2002) estimates of snow extent and water equivalent over central North America, *J. Hydrometeorol.*, 5, 850–861, [https://doi.org/10.1175/1525-7541\(2004\)005<0850:MCAPME>2.0.CO;2](https://doi.org/10.1175/1525-7541(2004)005<0850:MCAPME>2.0.CO;2), 2004.

440

Derksen, C., Lemmetyinen, J., Toose, P., Silis, A., Pulliainen, J., and Sturm, M.: Physical properties of Arctic versus subarctic snow: Implications for high latitude passive microwave snow water equivalent retrievals, *J. Geophys. Res. - Atmospheres*, 119, 7254–7270, <https://doi.org/10.1002/2013JD021264>, 2014.

445 Derksen, C. and Nagler, T.: ESA CCI+ Snow ECV: User Requirements Document, version 1.0, January 2019.

Durand, M., Kim, E., Margulis, S., and Molotch, N.: A first-order characterization of errors from neglecting stratigraphy in forward and inverse passive microwave modeling of snow, *IEEE Geosci. Remote S. Lett.*, 8, 730–734, <https://doi.org/10.1109/LGRS.2011.2105243>, 2011.

450

Durand, M., and Liu, D.: The need for prior information in characterizing snow water equivalent from microwave brightness temperatures, *Remote Sens. Environ.*, 126, 248–257, <https://doi.org/10.1016/j.rse.2011.10.015>, 2012.

455 Dyer, J., and Mote, T.: Spatial variability and trends in observed snow depth over North America. *Geophys. Res. Lett.*, 33, <https://doi.org/10.1029/2006GL027258>, 2006.

Forman, B. A., and Reichle, R. H.: Using a support vector machine and a land surface model to estimate large-scale passive microwave brightness temperatures over snow-covered land in North America, *IEEE Journal of Selected Topics in Applied Earth Observations and Remote Sensing*, 8, 4431–4441, <https://doi.org/10.1109/JSTARS.2014.2325780>, 2014.

460

Foster, J. L., Sun, C., Walker, J. P., Kelly, R., Chang, A., Dong, J., and Powell, H.: Quantifying the uncertainty in passive microwave snow water equivalent observations, *Remote Sens. Environ.*, 94, 187–203, <https://doi.org/10.1016/j.rse.2004.09.012>, 2005.



465 Gelaro, R., McCarty, W., Suárez, M. J., Todling, R., Molod, A., Takacs, L., Randles, C. A., Darmenov, A., Bosilovich, M. G., Reichle, R., Wargan, K., Coy, L., Cullather, R., Draper, C., Akella, S., Buchard, V., Conaty, A., da Silva, A. M., Gu, W., Kim, G., Koster, R., Lucchesi, R., Merkova, D., Nielsen, J. E., Partyka, G., Pawson, S., Putman, W., Rienecker, M., Schubert, S. D., Sienkiewicz, M., and Zhao, B.: The Modern-Era Retrospective Analysis for Research and Applications, Version 2 (MERRA-2), *J. Climate*, 30, 5419–5454. <https://doi.org/10.1175/JCLI-D-16-0758.1>, 2017.

470

Hall, D.: Influence of depth hoar on microwave emission from snow in northern Alaska, *Cold Reg. Sci. Technol.*, 13, 225–231, [https://doi.org/10.1016/0165-232X\(87\)90003-6](https://doi.org/10.1016/0165-232X(87)90003-6), 1987.

Hall, D., Sturm, M., Benson, C., Chang, A., Foster, J., Garbeil, H., and Chacho, E.: Passive microwave remote and in situ
475 measurements of Arctic and Subarctic snow covers in Alaska, *Remote Sens. Environ.*, 38, 161–172, [https://doi.org/10.1016/0034-4257\(91\)90086-L](https://doi.org/10.1016/0034-4257(91)90086-L), 1991.

Henn, B., Newman, A., Livneh, B., Daly, C., and Lundquist, J.: An assessment of differences in gridded precipitation datasets in complex terrain, *J. Hydrol.*, 556, 1205–1219, <https://doi.org/10.1016/j.jhydrol.2017.03.008>, 2018.

480

Kelley, R. E., Change, A. T., Tsang, L., and Foster, J. L.: A prototype AMSR-E global snow area and snow depth algorithm, *IEEE Trans. Geosci. Remote S.*, 41, 230–242, <https://doi.org/10.1109/TGRS.2003.809118>, 2003.

Kelly, R.E.J.: The AMSR-E Snow Depth Algorithm: Description and Initial Results, *Journal of the Remote Sensing Society of Japan*, 29, 307–317, <https://doi.org/10.11440/rssj.29.307>, 2009.
485

Krenke, A. Edited by National Snow and Ice Data Center. Former Soviet Union Hydrological Snow Surveys, 1966–1996, Version 1. Boulder, Colorado USA. NSIDC: National Snow and Ice Data Center. <https://10.7265/N58C9T60>, 1998, updated 2004.

490

Krinner, G., Derksen, C., Essery, R., Flanner, M., Hagemann, S., Clark, M., Hall, A., Rott, H., Brutel-Vuilmet, C., Kim, H., Ménard, C. B., Kim, H., Ménard, C. B., Mudryk, L., Thackeray, C., Wang, L., Arduini, G., Balsamo, G., Bartlett, P., Boike, J., Boone, A., Chéruy, F., Colin, J., Cuntz, M., Dai, Y., Decharme, B., Derry, J., Ducharne, A., Dutra, E., Fang, X., Fierz, C., Ghattas, J., Gusev, Y., Haverd, V., Kontu, A., Lafaysse, M., Law, R., Lawrence, D., Li, W., Marke, T., Marks, D., Ménégoz, M., Nasonova, O., Nitta, T., Niwano, M., Pomeroy, J., Raleigh, M. S., Schaedler, G., Semenov, V., Smirnova, T. G., Stacke, T., Strasser, U., Svenson, S., Turkov, D., Wang, T., Wever, N., Yuan, H., Zhou, W., and Dan Zhu, D.: ESM-SnowMIP:
495



assessing snow models and quantifying snow-related climate feedbacks, *Geosci. Model Dev.*, 11, 5027–5049, <https://doi.org/10.5194/gmd-11-5027-2018>, 2018.

500 Larue, F., Royer, A., De Sève, D., Langlois, A., Roy, A. and Brucker, L.: Validation of GlobSnow-2 snow water equivalent over Eastern Canada, *Remote Sens. Environ.*, 194, 264–277, <https://doi.org/10.1016/j.rse.2017.03.027>, 2017.

Lemmetyinen, J., Kontu, A., Kärnä, J.-P. , Vehviläinen, J. , Takala, M.,and Pulliainen, J.: Correcting for the influence of frozen lakes in satellite microwave radiometer observations through application of a microwave emission model, *Remote Sens. Environ.*, 115, 3695–3706, <https://doi.org/10.1016/j.rse.2011.09.008>, 2011.

505

Li, D., Durand, M., and Margulis, S.: Potential for hydrologic characterization of deep mountain snowpack via passive microwave remote sensing in the Kern River basin, Sierra Nevada, USA, *Remote Sens. Environ.*, 125, 34–48, <https://doi.org/10.1016/j.rse.2012.06.027>, 2012.

510

Liston, G., and Hiemstra, C.: The changing cryosphere: pan-Arctic snow trends (1979–2009), *J. Climate*, 24, 5691–5712, <https://doi.org/10.1175/JCLI-D-11-00081.1>, 2011.

Long, D., and Brodzik, M.-J.: Optimum image formation for spaceborne microwave radiometer products. *IEEE Geosci. Remote S.*, 54, 2763–2779, <https://doi.org/10.1109/TGRS.2015.2505677>, 2016.

515

Lundquist, J.D., Hughes, M., Henn, B., Gutmann, E.D., Livneh, B., Dozier, J., and Neiman, P.: High-elevation precipitation patterns: using snow measurements to assess daily gridded datasets across the Sierra Nevada, California, *J. Hydrometeorol.*, 16, 1773–1792, <https://doi.org/10.1175/JHM-D-15-0019.1>, 2015.

520

Markus, T., Powell, D., and Wang, J.: Sensitivity of passive microwave snow depth retrievals to weather effects and snow evolution, *IEEE Geosci. Remote S.*, 44, 68–77, <https://doi.org/10.1109/TGRS.2005.860208>, 2006.

Mudryk, L., Derksen, C., Kushner, P., and Brown, R.: Characterization of Northern Hemisphere snow water equivalent datasets, 1981–2010, *J. Climate*, 28, 8037–8051, <https://doi.org/10.1175/JCLI-D-15-0229.1>, 2015.

525

Mudryk, L., Kushner, P., Derksen, C., and Thackeray, C.: Snow cover response to temperature in observational and climate model ensembles, *Geophys. Res. Lett.*, 44, 919–926, <https://doi.org/10.1002/2016GL071789>, 2017.



530 Mudryk, L., Derksen, C., Howell, S., Laliberté, F., Thackeray, C., Sospedra-Alfonso, R., Vionnet, V., Kushner, P., and Brown, R.: Canadian snow and sea ice: historical trends and projections, *The Cryosphere*, 12, 1157–1176, <https://doi.org/10.5194/tc-12-1157-2018>, 2018a.

Mudryk, L., Brown, R., Derksen, C., Luoju, K., Decharme, B., and Helfrich, S.: Terrestrial Snow Cover [in Arctic Report
535 Card], 28 November 2018, <https://www.arctic.noaa.gov/Report-Card>, 2018b.

Mudryk, L., Brown, R., Derksen, C., Luoju, K., and Dechame, B.: Terrestrial Snow Cover [in: “State of the Climate 2018”], *Am. Meteorol. Soc.*, 100, S181–S185, <https://doi.org/10.1175/2019BAMSSStateoftheClimate.1>, 2019.

540 Neumann, N., Smith, C., Derksen, C., and Goodison, B.: Characterizing local scale snow cover using point measurements, *Atmos.-Ocean*, 44, 257–269, <https://doi.org/10.3137/ao.440304>, 2006.

Painter, T., Berisford, D., Boardman, J., Bormann, K., Deems, J., Gehrke, F., Hedrick, A., Joyce, M., Laidlaw, R., Marks, D.,
Mattmann, C., McGurk, B., Ramirez, P., Richardson, M., Skiles, S. M., Seidel, F., and Winstral, A.: The Airborne Snow
545 Observatory: Fusion of scanning lidar, imaging spectrometer, and physically-based modeling for mapping snow water
equivalent and snow albedo, *Remote Sens. Environ.*, 184, 139–152, <https://doi.org/10.1016/j.rse.2016.06.018>, 2016.

Pulliaainen, J.: Mapping of snow water equivalent and snow depth in boreal and sub-arctic zones by assimilating space-borne
microwave radiometer data and ground-based observations, *Remote Sens. Environ.*, 101, 257–269,
550 <https://doi.org/10.1016/j.rse.2006.01.002>, 2006.

Rawlins, M.A., Fahnestock, M., Frolking, S. and Vörösmarty, C.J.: On the evaluation of snow water equivalent estimates over
the terrestrial Arctic drainage basin, *Hydrol. Process.*, 21, 1616–1623, <https://doi.org/10.1002/hyp.6724>, 2007.

555 Rienecker, M. M., Suarez, M. J., Gelaro, R., Todling, R., Bacmeister, J., Liu, E., Bosilovich, M. G., Schubert, S. D., Takacs,
L., Kim, G., Bloom, S., Chen, J., Collins, D., Conaty, A., da Silva, A., Gu, W., Joiner, J., Koster, R. D., Lucchesi, R., Molod,
A., Owens, T., Pawson, S., Pegion, P., Redder, C. R., Reichle, R., Robertson, F. R., Ruddick, A. G., Sienkiewicz, M., and
Woollen, J.: MERRA: NASA’s Modern-Era Retrospective Analysis for Research and Applications, *J. Climate*, 24, 3624–
3648, <https://doi.org/10.1175/JCLI-D-11-00015.1>, 2011.

560

Rodell, M., Houser, P. R., Jambor, U. E. A., Gottschalck, J., Mitchell, K., Meng, C. J., Arsenault, K., Cosgrove, B.,
Radakovich, J., Bosilovich, M., Entin, J. K., Walker, J. P., Lohmann, D., and Toll, D.: The global land data assimilation system,
B. Am. Meteorol. Soc., 85, 381–394, <https://doi.org/10.1175/BAMS-85-3-381>, 2004.



565 Rott, H., Yueh, S. H., Cline, D. W., Duguay, C., Essery, R., Haas, C., Hélière, F., Kern, M. G., Malnes, E., Nagler, T., Pulliainen, J., Rebhan, H., and Thompson, A.: Cold regions hydrology high-resolution observatory for Snow and Cold Land Processes, *Proc. IEEE*, 98, 752–765, <https://doi.org/10.1109/JPROC.2009.2038947>, 2010.

Sospedra-Alfonso, R., Mudryk, L., Merryfield, W., and Derksen, C.: Representation of snow in the Canadian seasonal to
570 interannual prediction system. Part I: Initialization, *J. Hydrometeorol.*, 17, 1467–1488, <https://doi.org/10.1175/JHM-D-14-0223.1>, 2016.

Sturm, M., Holmgren, J. , and Liston, G.: A seasonal snow cover classification system for local to global applications, *J. Climate*, 8, 1261–1283, [https://doi.org/10.1175/1520-0442\(1995\)008<1261:ASSCCS>2.0.CO;2](https://doi.org/10.1175/1520-0442(1995)008<1261:ASSCCS>2.0.CO;2), 1995.

575

Sturm, M., Taras, B. , Liston, G. , Derksen, C. , Jonas, T. , and Lea, J.: Estimating snow water equivalent using snow depth data and climate classes, *J. Hydrometeorol.*, 11, 6, 1380–1394, <https://doi.org/10.1175/2010JHM1202.1>, 2010.

Takala, M., Luojus, K., Pulliainen, J., Derksen, C., Lemmetyinen, J., Kärnä, J.-P. ,and Koskinen, J.: Estimating northern
580 hemisphere snow water equivalent for climate research through assimilation of space-borne radiometer data and ground-based measurements, *Remote Sens. Environ.*, 115, 3517–3529, <https://doi.org/10.1016/j.rse.2011.08.014>, 2011.

Takala, M., Ikonen, J., Luojus, K., Lemmetyinen, J., Metsämäki, S., Cohen, J., Arslan, A. N., and Pulliainen, J.: New snow water equivalent processing system with improved resolution over Europe and its applications in hydrology, *IEEE Journal of Selected Topics on Applied Remote Sensing*, 10, 428–436, <https://doi.org/10.1109/JSTARS.2016.2586179>, 2017.

585

Tedesco, M., Kelly, R., Foster, J. L., and Change, A. T.: AMSR-E/Aqua Daily L3 Global Snow Water Equivalent EASE-Grids, Version 2. Boulder, Colorado USA, NASA Snow and Ice Data Center Distributed Active Archive Center, https://doi.org/10.5067/AMSR-E/AE_DYSNO.002, 2004.

590

Tedesco, M., and Narvekar, P.: Assessment of the NASA AMSR-E SWE product, *IEEE Journal of Selected Topics in Applied Earth Observations and Remote Sensing*, 3, 141–159, <https://doi.org/10.1109/JSTARS.2010.2040462>, 2010.

Tedesco, M., and Jeyaratnam, J.: A new operational snow retrieval algorithm applied to historical AMSR-E brightness
595 temperatures, *Remote Sensing*, 8, 1037, <https://doi.org/10.3390/rs8121037>, 2016.



Vuyovich, C. M., Jacobs, J. M., and Daly, S. F.: Comparison of passive microwave and modeled estimates of total watershed SWE in the continental United States, *Water Resour. Res.*, 50, 9088–9102. <https://doi.org/10.1002/2013WR014734>, 2014.

600 Wrzesien, M. L., Durand, M. T., Pavelsky, T. M., Kapnick, S. B., Zhang, Y., Guo, J., and Shum, C. K.: A new estimate of North American mountain snow accumulation from regional climate model simulations, *Geophys. Res. Lett.*, 45, 1423–1432, <https://doi.org/10.1002/2017GL076664>, 2018.